

Vibrational Raman modes and particle size analysis of cupric oxide with calcination temperature

M R Joya^{a*}, J Barba-Ortega^a & A M Raba^b

^aDepartamento de Física, Universidad Nacional de Colombia Bogotá, Carrera 30 Calle 45-03, CP 111321, Bogotá, Colombia

^bDepartamento de Física, Universidad Francisco de Paula Santander Cúcuta, avenue Gran Colombia 12E-96, Colombia

Received 16 November 2017; accepted 26 December 2018

In this work a study of the effect of the synthesis conditions on the vibratory and particle size properties in the cupric oxide (CuO) has been presented. The synthesis has been carried out by the polymeric precursor method without modifying the PH in the process, this being a low cost method. The samples obtained have been subjected to several calcination temperatures, 450 °C, 550 °C, 650 °C and 800 °C. In particle analysis by X-ray, scanning electron microscopy (SEM) and statistical it has been observed that for very low or very high calcination temperatures the particle size increases, finding 650 °C as the best calcination temperature. In the Raman spectra, the Ag and Bg vibration have been presented in the samples, with the peaks being narrower for the temperature of 450 °C.

Keywords: Synthesis, Cupric, Particle, Spectroscopy

1 Introduction

Copper oxide (CuO) is one of *p*-type semiconductors with an indirect band gap and gains considerable attentions due to its excellent optical, electrical, physical, and magnetic properties. The CuO is extensively used in various applications such as catalysis, solar energy conversion, gas sensor and field emission¹. In particular, the two main copper oxide phases, which are cupric (CuO) and cuprous (Cu₂O) oxide, are considered among the most important semiconductors with a band gap E_g in the range of 1.72-2 eV. In addition to cupric and cuprous oxide, an interesting intermediate phase, paramelaconite Cu₄O₃ is found in the literature^{2,3}.

It has been reported in the literature of the synthesis of CuO nanocrystals, Cu₂O modulating the morphology, temperature, free environment, the use of surfactants and the dependence of the organic catalytic activity with the shape of the nanoparticles. A chemical route free of surfactants for the manufacture of nanotubes, octahedra, spheres, plates and polyhedra of Cu₂O by varying the reaction atmosphere. Apparently oxygen adsorption and reactions on the surface of Cu₂O may be able to slow Cu(OH)₂ reduction and Cu₂O nucleation and also exert a remarkable influence on growth³⁻⁷.

The CuO has been studied extensively in the literature, in terms of its vibrational modes, with variations in the shifting of its peaks by the effect of annealing of samples. CuO has 12 phonon branches because there are four atoms in the primitive cell. A factor-group analysis gives the following zone-center modes.

$$\tau = Ag + 2Bg + 4Au + 5Bu \quad \dots (1)$$

The three acoustic modes are of Au+2Bu symmetry. Among the nine optical modes, three (Ag+2Bg) are Raman-active, and the remaining six (3Au+3Bu) are IR-active^{2,8-12}. In the present study, we report the synthesis of CuO nanoparticles at different calcination temperatures. The final samples were characterized by means of Raman spectroscopy, X-rays and SEM. The synthesis shows that very low temperatures or high calcination temperatures affect the size of the nanostructures. In the present work, the main objective is to investigate the effect of starting precursors on structural properties of CuO nanostructures synthesized via precipitation method and annealing process.

2 Materials and Methods

The powder was obtained by the Pechini method. Initially, at 20% aqueous solution of cupric chloride dehydrate (CuCl₂·2H₂O-Panreac 99.8%) was prepared, which contained 23.3518g of solute.

*Corresponding author (E-mail: mrinconj@unal.edu.co)

Simultaneously, an aqueous solution 20% of citric acid monohydrate (Panreac 99.8%) was prepared, which contained 88.1285g of it. The two solutions were mixed under constant agitation maintaining a temperature of 80 °C for half an hour. In this mixture, 52.7873 mL of ethylene glycol (Panreac 99.8%) was added at 90 °C. This temperature remained, until reduced the volume of water. The obtained resin is precalcined at 300 °C, at 150 °C and finally at 300 °C, in order to remove solvents still present, the result of these precalcineds was macerated using an agate mortar. The resulting material is initially sieved in No. 20 sieve (850µm pore size), then in No. 50 sieve (300µm pore size). The powders after the sieved were subjected to thermal treatments recorded in Table 1. The precalcining conditions of the samples were as follows; 300 °C (4 h rising to 1.1 °C/min and 1 h in plateau), 150 °C (4 h rising to 0.5 °C/min and 2 h in plateau) and finally 300 °C (4 h in ascent at 1.1 °C/min and 2 h in plateau).

The XRD patterns of the samples synthesized via the two methods were obtained using Panalytical PW3373 equipment (CuK α_1 radiation, $\lambda = 1.540558$ Å), operating at 40 mA with a step of 0.05° for 50 s. The 2 θ angle range of 5-80° was used. The identification of the crystalline phases was carried out using the X'Pert software HighScore PANalytical. The morphological characterization of the samples, measured in SEM, were performed using a microscope VEGA3 SB with a tungsten filament, an accelerating voltage of 5 kV in low vacuum conditions and it has a detector XFlash Detector 410M. The Software ImageJ was used for nanoparticle size distribution analysis. Raman spectroscopy was made using a commercial micro-Raman probe setup TG4000 Jobin Yvon spectrometer (Raman excitation line: $\lambda = 632\text{nm}$) at room temperature.

3 Results and Discussion

The XRD patterns of as-synthesized and calcined CuO nanoparticles using different precursors are shown in Fig. 1. XRD peaks confirm that the

Table 1 – Final thermal treatment of precalcined samples.

T (°C)	Heating ramp (°C/min)	Ascent time (h)	Plateau time (h)	Initial mass (g)	Final mass (g)
450	3.5	2	2	1.207	0.166
550	4.4	2	2	1.201	0.120
650	5.2	2	2	1.206	0.160
800	4.3	2	0.5	1.409	0.196

formation of CuO from each precursor was in monoclinic phase. The characteristic peaks located at 2 $\theta = 32.5^\circ$, 35.6°, 38.5°, 48.85° and 53.49° are assigned to (110), (-111), (111), (-202) and (020) among others.

Figure 1 shows diffractograms of the samples submitted at (a) 650 °C and (b) 800 °C. The Tenorite phase of the CuO was identified contrasts our results with the stored ones in power diffraction file. The card No. 01-072-0629 ($a = 4.6837$ Å, $b = 3.4226$ Å and $c = 5.1288$ Å) was found for the two cases, with structure monoclinic showing that the symmetry is C_2/c . No reflections related to any secondary phase are detected in the diffractograms. The crystallite sizes were estimated using the Scherrer equation for the peak of maximum intensity. For the sample submitted at 650 °C was obtained a crystallite size of 109.43 nm and for the sample submitted at 800 °C was obtained a value of 110.98 nm.

SEM micrographs show changes in morphology with increasing temperature values. Samples prepared and sintered at temperature of 450 °C, 550 °C, 650 °C and 800 °C, a shape of spheres and plates is observed. The SEM micrograph clearly showed the agglomeration of nanostructures. In Fig. 2 (a) at temperature of 450 °C, the shape in the morphology of the particles is of plates and some rhombohedral. In this figure, it is observed that the sizes of the particles vary, there is no uniformity in them. However, for Fig. 2(b,c) the morphology of the particles is more homogeneous. For temperatures of 450 °C and 800 °C the particle size was more irregular compared to Fig. 2(b,c). The smallest

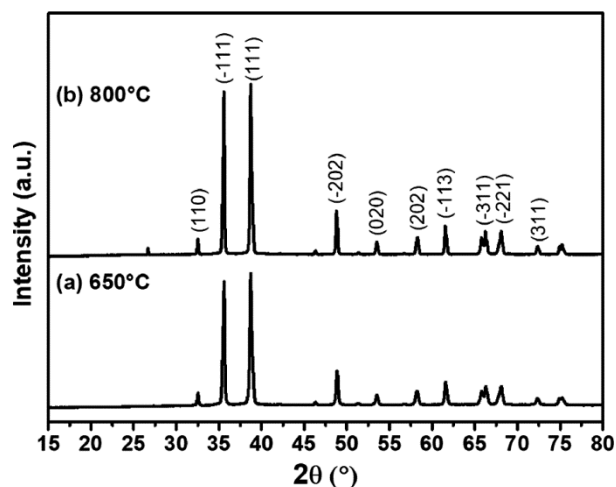


Fig. 1 – XRD pattern of synthesized CuO nanoparticles at temperatures of 650 °C and 800 °C.

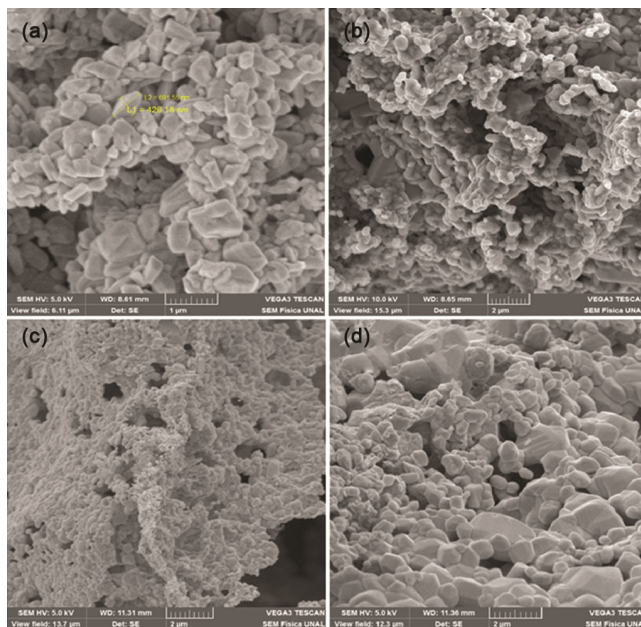


Fig. 2 – SEM image of CuO nanoparticles; (a) 450 °C, (b) 550 °C, (c) 650 °C and (d) 800 °C.

particle size seems to be for the sample at 650 °C. While the particle size for the temperature of 800 °C of Fig. 2(d) increased. Nevertheless, although the increase in calcination temperature improves the particle size, there is a limit where the particle size begins to increase. For the samples of this study it can be said that the calcination temperature limit is between 600 °C and 700 °C. ImageJ is software for image analysis with which the film size of the calcined samples, were analyzed at temperatures of 450 °C and 650 °C. In the histogram of Fig. 3(a) the irregularity of the particle size is observed.

Making use of the statistical part, it was found that the mean for the particles is 157.23 nm. In Fig. 3(b) at a calcination temperature of 650 °C the mean particle size was 152.7 nm. Comparing this last sample with the data obtained in X-rays, it can be said that the particle size increases with the increase in temperature. However, to obtain values closer to the particle size by X-rays and statistical analysis, a larger particle count is necessary. In a comparative analysis in X-rays, SEM and the statistic, it is observed that the calcination temperature affects the uniformity and the size of the particle in the samples.

In the Ag and Bg Raman modes only the oxygen atoms move, with displacements in the b-direction for Ag and perpendicular to the b-axis for Bg modes. The infrared active modes involve the motion of both the O and the Cu atoms. The induced dipole

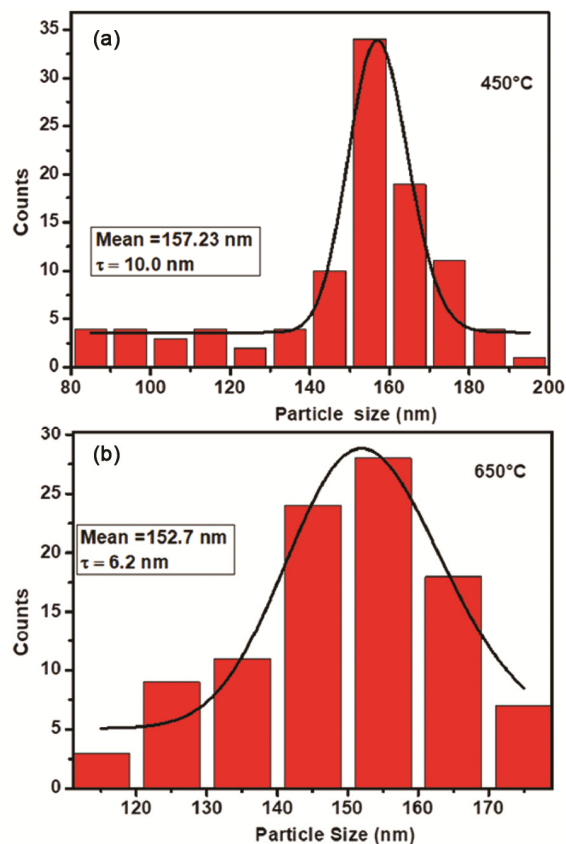


Fig. 3 – Counts of particles versus size the particle. In a count of 100 particles, the mean size is (a) 157.23 nm. Sample calcined at 450 °C for 2 h and (b) mean size is 152.7 nm. Sample calcined at 650 °C for 2 h.

moment is along the b-axis for the Au modes and perpendicular to it for the Bu modes⁸⁻¹¹. The position of the Raman peaks of Fig. 4 was found with the Peak Fit software. Finding the position of the Raman peaks, in this paper and comparing them with those calculated theoretically from the literature, we find the following; calculation of phonon frequencies for Tenorite CuO, Ag(296cm⁻¹), Bg (346cm⁻¹) and Bg (631cm⁻¹)¹². In this work in figure 4 the position of the peaks for the sample calcined to 450°C was: Ag (286cm⁻¹), Bg (335 cm⁻¹), Bg (625 cm⁻¹) and for sample to 650°C; Ag (281 cm⁻¹), Bg (329cm⁻¹), Bg (610cm⁻¹).

Comparing the position of the Raman frequencies of the two experimental samples of this work and the theory, it is evident that the closest results are for the sample annealed at 450 °C. This indicates that the calcination of the samples increases, the position of the Raman peaks decreases. The variation of the position can be influenced by the number of defects in the samples.

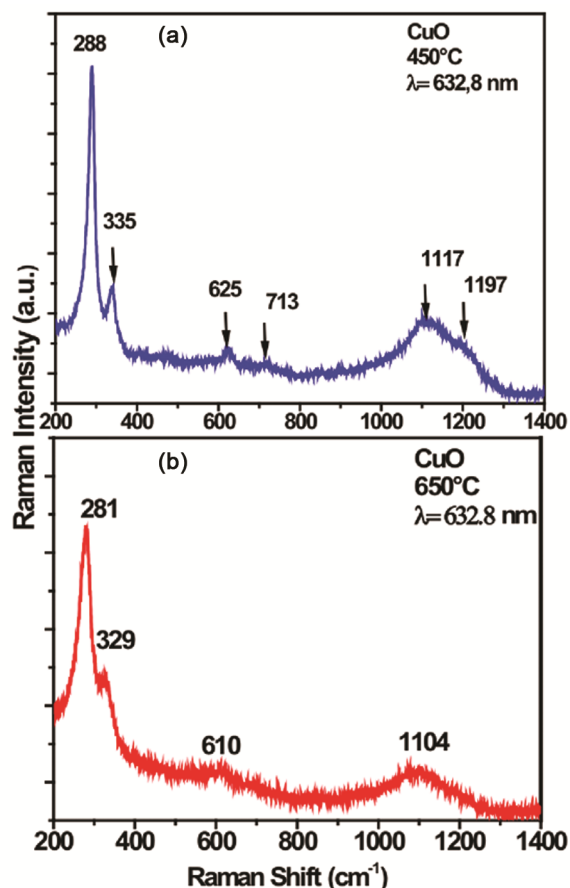


Fig. 4 – Raman spectra of the as prepared samples (a) 450 °C and (b) 650 °C.

4 Conclusions

In summary, CuO nanostructures were successfully synthesis by polymeric precursor method obtain the cupric oxide. XRD, SEM and Raman spectrum

results suggest that the better formation of CuO nanostructures can be attained for calcination temperatures between 600 °C and 700 °C. At a higher temperature, the Raman peak changes to a smaller wave number and broadens. The difference of the Raman spectra of the CuO nanocrystals is mainly due to the particle size effects.

Acknowledgement

The financial support is sincerely appreciated from the agencies Colciencias-Colombia and from the University Francisco de Paula Santander Cúcuta Colombia, National university of Colombia Bogotá.

References

- 1 Phiwdang K, Suphankij S, Mekprasart W & Pecharapa W, *Energy Procedi*, 34 (2013) 740.
- 2 Debbichi L, Marco de Lucas M C, Pierson J F & Kruger P, *J Phys Chem C*, 116 (2012) 10232.
- 3 Suleiman M, Mousa M, Hussein A, Hammouti B, Hadda T B & Warad I, *J Mater Environ Sci*, 4 (2013)792.
- 4 Song J, Xu L, Zhou C, Xing R, Dai Q, Liu D & Song H, *ACS Appl Mater Interfaces*, 5 (2013) 12928.
- 5 Kozak D S, Sergiienko R A, Shibata E, Iizuka A & Nakamura T, *Sci Rep*, 6 (2016) 21178.
- 6 Joya M R, Raba A M & Barba-Ortega J, *Respuestas*, 21 (2016) 89.
- 7 Joya M R, Raba A M & Barba-Ortega J, *Universidad Cienciay Tecnol*, 20(2017) 188.
- 8 Xu J F, Ji W, Shen Z X, Li W S, Tang S H, Ye X R Jia, D Z & Xin X Q, *J Raman Spectrosc*, 30 (1999) 413.
- 9 Sardari B & Zcan M, *Sci Rep*, 7 (2017) 7730.
- 10 Gan Z H, Yu G Q, Tay B K, Tan C M, Zhao Z W & Fu Y Q, *J Phys D: Appl Phys*, 37 (2004) 81.
- 11 Tohidi S H, Novinrooz A J, Derhambakhsh M & Grigoryan G L, *Int J Nanosci Nanotechnol*, 8 (2012) 143.
- 12 Colomban P & Schreiber H D, *J Raman Spectros*, 36 (2005) 884.